Forest Ecology and Management xxx (2012) xxx–xxx

Contents lists available at SciVerse ScienceDirect

Forest Ecology and Management

journal homepage: www.elsevier.com/locate/foreco

Future U.S. wildfire potential trends projected using a dynamically downscaled climate change scenario

Yongqiang Liu *, Scott L. Goodrick, John A. Stanturf

Center for Forest Disturbance Science, US Forest Service, 320 Green St., Athens, GA 30602, United States

ARTICLE INFO

Article history:
Available online xxxx

Keywords:
Wildfire
Climate change
Keetch–Byram Drought Index (KBDI)
modified Fosberg Fire Weather Index (mFFWI)
Continental U.S.

ABSTRACT

This study investigates trends in wildfire potential in the continental United States under a changing climate. Fire potential is measured by the Keetch–Byram Drought Index (KBDI), which is determined by daily maximum temperature and precipitation. The impact of relative humidity and wind speed is examined by comparing KBDI with the modified Fosberg Fire Weather Index (mFFWI). The present (1971–2000) and future (2041–2070) daily regional climate conditions were obtained by dynamical downscaling of the HadCM3 global projection using HRM3 regional climate model provided by the North America Regional Climate Change Assessment Program (NARCCP). It is shown that fire potential is expected to increase in the Southwest, Rocky Mountains, northern Great Plains, Southeast, and Pacific coast, mainly caused by future warming trends. Most pronounced increases occur in summer and autumn. Fire seasons will become longer in many regions. The future fire potential increase will be less pronounced in the northern Rocky Mountains due to the changes in humidity and wind. Present fire potential is found to have been increasing across continental U.S. in recent decades. The future KBDI increase in the central Plains and the South projected using the HadCM3–HRM3 climate change scenario is smaller than the increases using the climate change scenarios from most of other NARCCAP model combinations. Larger inter-seasonal and inter-annual fire potential variability is expected in the future in the Pacific and Atlantic coastal regions. The projected increases in wildfire potential for many regions of the U.S. suggest that increased resources and management efforts for disaster prevention and recovery would be needed in the future.

1. Introduction

Periodic wildfires are characteristic of fire-adapted ecosystems worldwide. Wildfires, meanwhile, can also be a major natural disaster. Increased fuel loading resulting from fire exclusion and other management activity, arson ignitions and expansion of human settlements into fire-prone vegetation driven by population growth have resulted in more frequent and costlier wildfires. About 370 M ha (1 M ha = 10^4 km^2, 1 ha = 2.47 acres) of forest and other ecosystems were burned globally each year on average during 1997–2008 (Giglio et al., 2010). The 1997–1998 fires in Indonesia burned 8 M ha (Cochrane, 2003). The latest catastrophic wildfires in southeastern Australia (AP, 2009) burned about 0.22 M ha of forest, destroyed 750 homes on 1 day, and killed more than 200 people. In the United States, almost 2 M ha of forest and other ecosystems were burned annually from 1992 to 2001, which cost billions of U.S. dollars (USFA, 2005). The burned areas increased to about 3 M ha from 2002 to 2011 (NIFC, http://www.nifc.gov/fireInfo/fireInfo_stats_totalFires.html).

Wildfires can also lead to adverse environmental consequences. Wildfires emitted about 2.0 Pg C annually during 1997–2009, about one third of the total carbon emissions (van der Werf et al., 2010). The carbon emissions from the 1997–1998 Indonesian wildfires were the equivalent of the total global carbon uptake by the terrestrial biosphere in a typical year (Page et al., 2002; Tacconi et al., 2007). Smoke particles are one source of atmospheric aerosols, which affect atmospheric radiative transfer through scattering and absorbing solar radiation and modifying cloud microphysics (Charlson et al., 1992; Forster et al., 2007). These processes can further modify clouds and precipitation and atmospheric circulations (Ackerman et al., 2000; Liu, 2005a, 2005b). Boreal fires are an important factor for greenhouse effect and radiative forcing. They contribute more black carbon to the Arctic than anthropogenic sources in summer (Stohl et al., 2006); the deposition of black carbon on snow and ice covers in high latitudes reduces albedo of snow and increases the solar radiation absorbed by the ground, which in turn speeds up snow melting (Hansen and Nazarenko, 2004). The roles of boreal fires in short- and long-terms climate variability could be different. Randerson et al. (2006), for example, indicated based on measurements and analysis of a boreal forest fire that the integrating the effects of greenhouse gases, aerosols,

* Corresponding author. Tel.: +1 706 559 4240; fax: +1 706 559 4317.
E-mail address: yliu@fs.fed.us (Y. Liu).

0378-1127/$ - see front matter Published by Elsevier B.V.
http://dx.doi.org/10.1016/j.foreco.2012.06.049

black carbon deposition on snow and sea ice, and postfire changes in surface albedo will increase radiative forcing during the first year, but to decrease radiative forcing when averaged over an 80-year fire cycle, implying that future increases in boreal fire may not accelerate climate warming. In addition, wildfires release large amounts of particulate matter (PM) and other air pollutants, which can degrade air quality (Riebau and Fox, 2001; Langmann et al., 2009).

Fire potential as well as fire behavior of individual fires during specific days or months is determined by fire weather, which is characterized by atmospheric elements such as temperature, humidity, wind and atmospheric processes such as precipitation, fronts, jet streams, and troughs/ridges. Temperature, humidity, wind speed, and precipitation can affect fuel moisture which is a factor for fire ignition, while wind is important for both fire ignition and spread. Fire activity during an entire fire season, inter-fire season variability, inter-annual variability, and long-term trends, meanwhile, are determined by fire climate, which is a synthesis of daily fire weather (Pyne et al., 1996). Fire climate describes statistical features (e.g., means and variances) of fire weather features over a long period.

The relationship between wildfire and climate has received increasing scrutiny in recent years due to occurrence of catastrophic mega-fires and potential effects of climate change on fire regimes (Flannigan et al., 2009a, 2009b; Wotton et al., 2010). There has been a trend for increased fire activity, especially catastrophic mega-fires, in recent decades (Piñol et al., 1998; UNFAO, 2001; Gillett et al., 2004; Reinhard et al., 2005; Westerling et al., 2006). Among the converging factors seen as underlying this trend were extreme weather events such as extended droughts (Goldhammer and Price, 1998; Stocks et al., 2003), which are persistent weather anomalies that can directly impact the fire activity of a fire season. Of additional concerns is possible impact on fire of climate change. Many climate models have projected significant climate change this century due to the greenhouse effect (IPCC, 2007), including an overall increase in temperature worldwide and a drying trend in many subtropical and mid-latitude regions. Thus, it is likely wildfires will increase in these regions. Understanding of future wildfire trends under projected climate change is essential to assessing wildfire's potential impacts and damage to humans, ecosystems and the environment in the future, and to further designing and implementing necessary measures to mitigate these impacts.

Several approaches to projecting fire trends are available. One is to use fire weather indices to project fire potential and risk, which is a measure of the possibility of fires of a certain severity occurring in an area. Some of the most popular indices are the Keetch–Byram Drought Index (KBDI) (Keetch and Byram, 1968), Fire Weather Index (FWI) (Van Wagner, 1987), energy release component (ERC), and the burning index (BI). Another approach is to build statistical relations between historical fire properties (burned areas, occurrence, intensity, severity, and seasonality, etc.) and fire weather indices or atmospheric elements (e.g., temperature, humidity, precipitation, and lightning), and project future fire properties based on projected future climate. Fuel conditions and human activity are also useful factors in addition to climate conditions. A third approach is vegetation modeling, often using dynamic global vegetation models (DGVMs) such as HYBRIDS (Friend et al., 1995), MC1 (Bachelet et al., 2001a, 2001b), LPJ (Sitch et al., 2003), CLM (Levis et al., 2004), IBIS (Foley et al., 2005), and DLEM (Tian et al., 2010).

These approaches have been used to project future global fire trends. Scholze et al. (2006) simulated changes in global ecosystem processes due to climate change with the LPJ model based on multiple scenarios from 16 climate models. Krawchuk et al. (2009) used statistical generalized additive models to characterize current fire patterns and project the potential distribution of future fire based on fire, climate, net primary productivity, and ignition data. Liu et al. (2010) projected global fire potential using the KBDI and future climate projections from four climate models under various emissions scenarios. Pechony and Shindell (2010) used empirical relations among fire activity and parameters including vegetation density, ambient meteorological conditions, availability of ignition sources, and fire suppression rates to project fire trends based on simulated climate variations and land-use changes. These studies projected increased future fire occurrence and severity in western North America, southern Europe, central Asia, and central South America, central South Africa, and parts of Australia.

More detailed projections of future fire trends for North America have been provided based on regional or local climate change scenarios downscaled statistically or dynamically from global climate model or general circulation model (GCM) projections. For Canada, Flannigan et al. (2001) showed that future forest fire danger measured by FWI is expected to increase in most of Canada although there is significant regional variability including a decrease in much of eastern Canada. Amiro et al. (2001), Flannigan et al. (2005), and Balshi et al. (2008) projected an overall increase in burned area of the boreal regions. Wotton and Martell (2005) projected an increase in lightning fire activity of 80% for Ontario, Canada by the end of the 21st century. For the U.S., Brown et al. (2004) showed that the number of days of high fire danger for the western U.S. measured using ERC will increase in the northern Rockies, Great Basin and the Southwest; Liu et al. (2005) estimated an increase of 50% in burned area for the continental U.S. and over 100% for the western U.S. by 2050, while Spracklen et al. (2009) estimated an increase of 54% for the western U.S. by that time. Many studies (e.g., Bachelet et al., 2001a, 2001b; Lenihan et al., 2003; Whitlock et al., 2003; Rogers et al., 2011) projected an increase in burned area across the U.S. using the MC1 dynamic vegetation model.

In an earlier study of global fire potential trends measured using the KBDI (Liu et al., 2010), the United States was identified as one of the geographic regions where significant increase in fire potential is expected under a changing climate in the future. In this study we provide further details of spatial patterns and temporal variations of future fire potential trends in the continental U.S. by using a dynamically downscaled regional climate change scenario prepared by the North America Regional Climate Change Assessment Program (NARCCAP) (Mearns et al., 2009). The next section describes the methods and data used for calculating KBDI and another fire index, the modified Fosberg Fire Weather Index. The results and discussion are provided in Sections 3 and 4, respectively. Conclusions are provided in the final section.

2. Data and methods

2.1. Regional climate scenario

The datasets of the present and future regional climate generated by NARCCAP (Mearns et al., 2009) were used. NARCCAP produces high-resolution climate change simulations to investigate uncertainties in regional scale projections of future climate and to generate climate change scenarios for use in climate change impact research. Regional climate change scenarios are obtained by running a set of regional climate models (RCMs) driven by a set of global general circulation models (GCMs) over North America. The GCMs used are the Community Climate System Model (CCSM), the Coupled Global Climate Model, version 3 (CGCM3), the Geophysical Fluid Dynamics Laboratory climate model (GFDL), and the Hadley Centre Climate Model, version 3 (HadCM3). The RCMs used are the Canadian Regional Climate Model (CRCM), the Regional Spectral Model (RSM), the High resolution Regional Model

(HRM), the Meso-scale Meteorological Model, version 5 (MM5I), the Regional Climate Model, version 3 (RCM3), and the Weather Research and Forecasting model (WRFG). There are total 10 GCM–RCM combinations.

Simulations were conducted for the present period of 1971–2000 and the future period of 2041–2070 at a spatial resolution of 50 km. The downscaling of future climate projections was made only for the IPCC Special Report on Emission Scenarios (SRES) A2 emissions scenario (Nakicenovic et al., 2000). A2 together with three other scenarios combines two sets of divergent tendencies: one set varies between strong economic values and strong environmental values, the other set between increasing globalization and increasing regionalization. In comparison with the A1 scenario that describes a future of very rapid economic growth, global population that peaks in mid-century and declines thereafter, and the rapid introduction of new and more efficient technologies, the A2 scenario describes a very heterogeneous world with slower growth and greater regional disparity.

The spatial patterns and seasonal variations of KBDI were calculated and analyzed in this study using the daily regional climate change scenario from the HadCM3–HRM3.

2.2. Keetch–Byram Drought Index (KBDI)

KBDI is in essence an indicator of soil moisture deficit and is based on a number of physical assumptions (Chu et al., 2002). Soil water transfer to the atmosphere through evapotranspiration is determined by temperature and annual precipitation, which is used as a surrogate for vegetation cover (areas with higher annual rainfall are assumed to support more vegetation). See Supplementary material for the formulas to calculate KBDI. KBDI was developed and evaluated for the southeastern U.S. It has been used for guidelines on expected fire conditions and potential suppression problems for this region (Melton, 1989). The applicability and possible limitations to other geographic regions were discussed in, for example, Snyder et al. (2006), Xanthopoulos et al. (2006), Groisman et al. (2007), and Liu et al. (2010). In general, KBDI has been found useful beyond the southeastern U.S.

Wildfire potential is divided into four levels based on KBDI values (http://www.wfas.net). (a) Low (KBDI = 0–200): Soil moisture and large class fuel moistures are high and do not contribute much to fire intensity. (b) Moderate (200–400): Lower litter and duff layers are drying and beginning to contribute to fire intensity. (c) High (400–600): Lower litter and duff layers contribute to fire intensity and will actively burn. (d) Extreme (600–800): Intense, deep burning fires with significant downwind spotting can be expected. The four KBDI levels are typical of spring dormant season following winter precipitation, late spring and early in the growing season, late summer and early autumn, and often associated with more severe drought and increased wildfire occurrence, respectively.

2.3. Fire potential projections and analyses

Daily KBDI was calculated for present and future periods, each with a period of 30 years, using the daily NARCCAP datasets. The calculation steps at each grid point are as follows: (1) Daily KBDI was calculated for first 5 years starting from an initial value of zero. (2) The average of the values on the last day of each year was obtained. (3) Daily KBDI was recalculated but for the entire 30 years using the average as an initial value.

Future fire potential trends were projected based on the calculated present and future KBDIs using the corresponding daily regional temperature and precipitation conditions from NARCCAP. To examine the relative importance of changes in the two meteorological variables, two more KBDI projections were made, one only considering future change in maximum temperature and the other only future change in precipitation.

One of the recognized limitations with KBDI is that it does not include humidity and wind, which are also closely related to fire occurrence and behavior (Flannigan and Harrington, 1988). To examine the impact of these two meteorological elements, the KBDIs were compared with the modified Fosberg Fire Weather Index (see Supplementary material).

The future fire potential trends were projected only using the regional climate change from HadCM3–HRM3. A very rough comparison of KBDI was made between this model combination with other combinations based on the data provided in Mearns (2012) (see Supplementary material).

3. Results

3.1. Present climate and future change

3.1.1. Temperature

The present maximum surface air temperature (Fig. S1) shows a spatial pattern of decreasing from about 25 °C in the subtropics (Florida, southern Texas, and southern California) to just below zero in the middle latitudes in winter. Temperature is slightly higher in the western than the eastern U.S. except in the Rocky Mountains where temperature is below −5 °C due to high elevation. Temperature increases in spring but the spatial pattern remains almost the same. Temperature further increases in summer, most remarkably in the southwestern U.S. It decreases from above 40 °C in this region to about 25 °C in northeastern U.S. The magnitude and pattern in autumn are similar to those in spring.

Future temperature is projected to increase almost everywhere in all seasons (Fig. 1). During winter and spring, only the higher latitudes show a large increase. This pattern totally changes in summer, when temperature in the central U.S. increases by more than 4 °C. The pattern in summer remains the same in the autumn but with reduced magnitude.

3.1.2. Precipitation

Present precipitation in winter (Fig. S2) occurs mainly in the eastern U.S. and along the Pacific coast as well as at some patchy locations in the Rocky Mountains. The magnitude of seasonal precipitation is more than 300 mm. The spatial pattern remains the same in spring, but the major precipitation areas expand in the eastern U.S. but retreat in the Pacific coast. In summer, the eastern precipitation area further expands, while the western one disappears. Seasonal precipitation amount is less than 30 mm in the Pacific coast and Intermountain. Precipitation pattern in autumn is characterized by the return of large amount of precipitation in the northern Pacific coast and small amount of precipitation in the Southeast.

Future winter precipitation (Fig. 2) is projected to increase. The largest increase occurs in the eastern U.S. with a magnitude of over 60 mm. In contrast, precipitation will decrease in the northern Pacific coast and southern Plains. Future precipitation decrease is more noticeable in spring, especially in the Southwest. The decreasing areas further expand to almost entire western U.S. in summer with a magnitude of about 50 mm, and to the Southeast in the autumn.

3.1.3. Relative humidity

Air relative humidity (RH) is directly proportional to air specific moisture, which often correlates well to precipitation, and inversely proportional to air temperature. The impact of temperature is clearly seen in winter RH, which shows a generally opposite

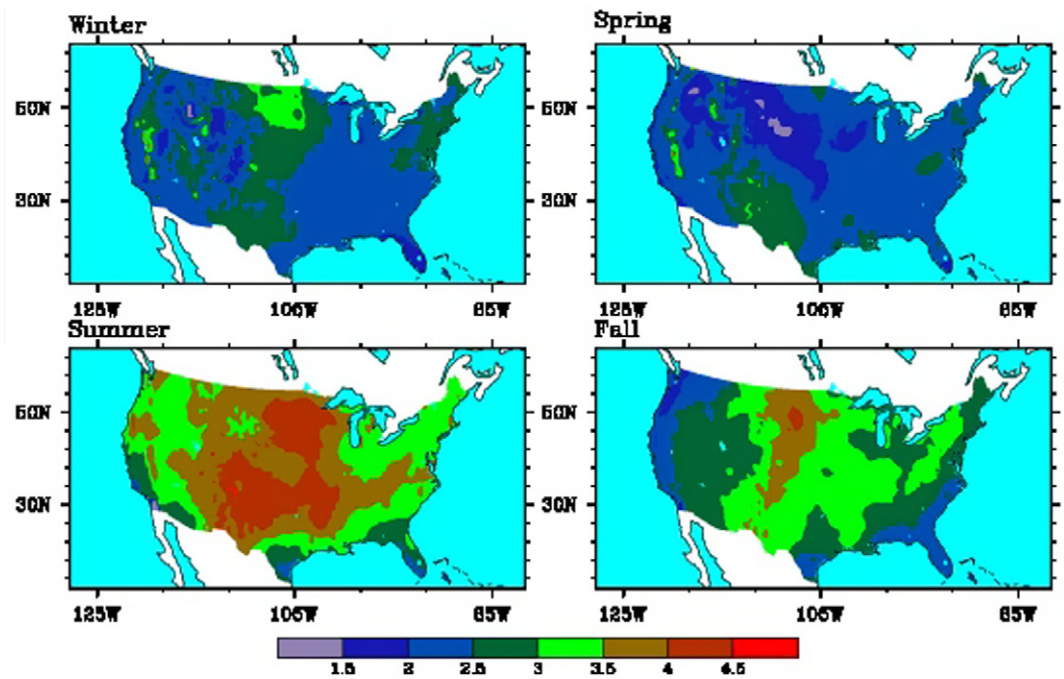

Fig. 1. Spatial patterns of future change in maximum air temperature in the continental U.S. (in °C) between 2041–2070 and 1971–2000. The four panels are for winter, spring, summer, and autumn. (The data used for this figure were obtained from the NARCCAP.)

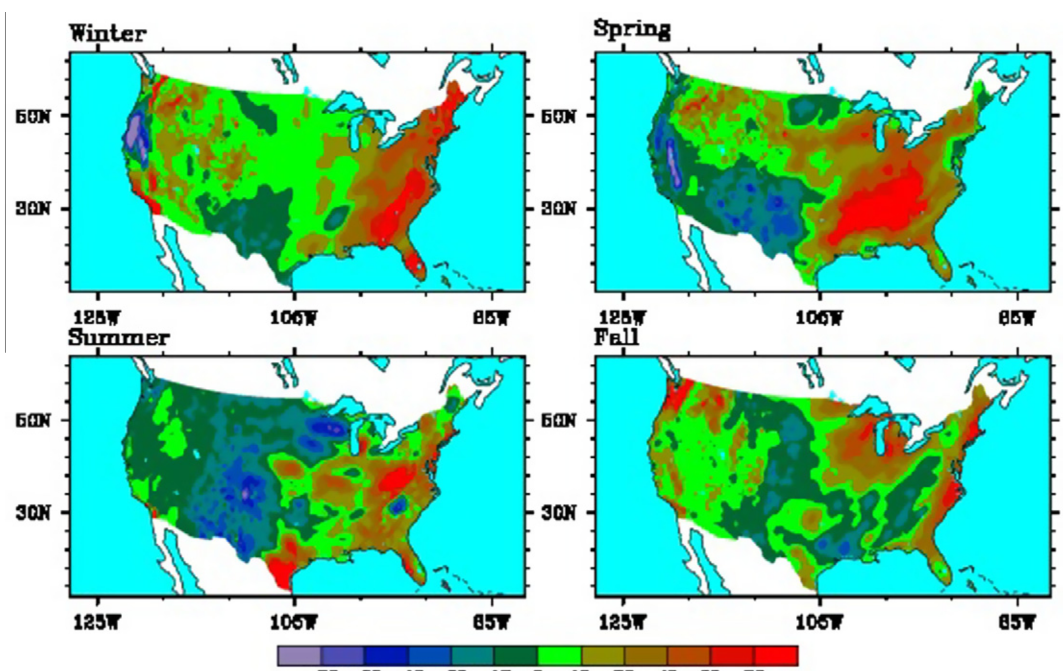

Fig. 2. Same as Fig. 1 except for precipitation (in mm).

spatial pattern to that of temperature. RH increases in winter from less than 40% in the southwestern U.S. to more than 90% in the northern Midwest and Northeast as well as in the Rocky Mountains (Fig. S3). Spring RH has a similar spatial pattern but smaller magnitude due to increased temperature from winter to spring. Summer RH increases from 20% to 30% in the Pacific coast and Intermountain (except for a narrow coastal band) to the 40s% in the Rocky Mountains, 50s% in the Great Plains, and 60s% in the Midwest and most of the eastern U.S. RH in autumn again shows an increasing trend relative to summer.

Future winter RH will decrease everywhere except some spots in the northwestern U.S. (Fig. 3). RH will decrease by 6% or more in parts of the Southwest and the Intermountain, and about 4% in the Great Plains and Appalachia. In spring, a large reduction is also seen in the Midwest. Summer RH decreases by 10% in the southern Rockies and western Midwest, but increases in California, southern

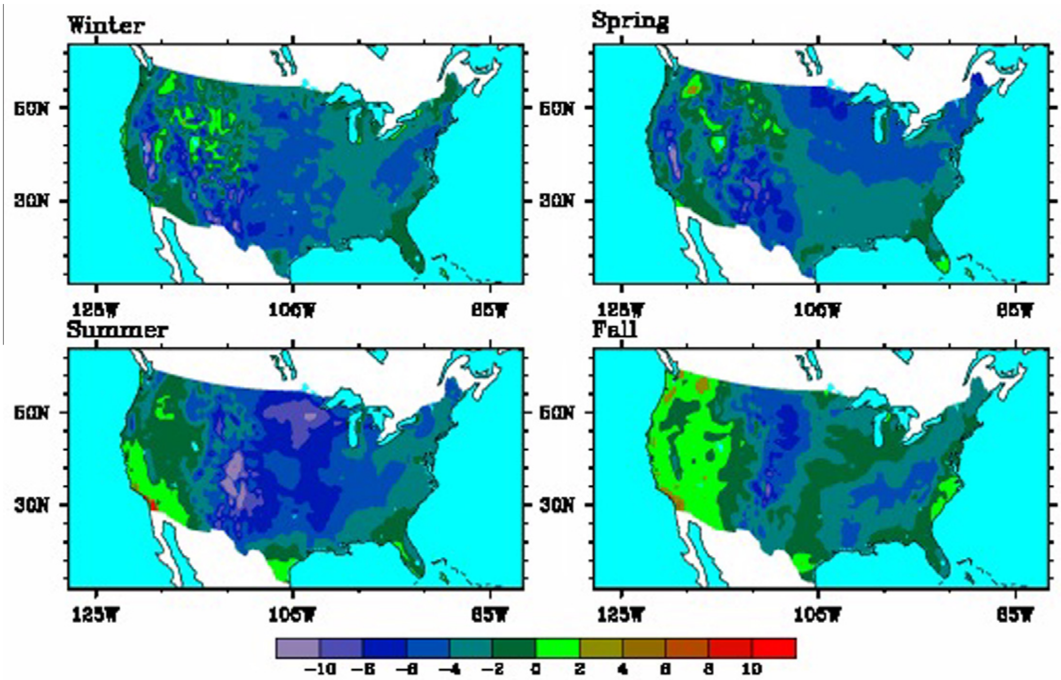

Fig. 3. Same as Fig. 1 except for surface air relative humidity (%).

Texas, and parts of Florida. The area with increased RH extends to the region west of the Rocky Mountains in the autumn.

3.1.4. Wind speed

Present wind speed has a similar spatial pattern throughout seasons, that is, relatively windy conditions in the Great Plains and Midwest and calm conditions in other regions (Fig. S4). The magnitude is the largest and smallest in spring and summer, respectively.

Future change in wind speed is also similar among various seasons except autumn (Fig. 4). Wind speed mostly decreases in the northern U.S. but increases in the southern U.S. in winter, spring, and summer. Wind speed in autumn decreases in the western U.S. and the southeastern coastal area, but increases in the Great Plains and Midwest.

3.2. KBDI

3.2.1. Spatial patterns

Fig. 5 shows spatial patterns of present KBDI values for individual seasons. In winter, a belt of large values over 600 (high fire potential) is found in the inland areas of the Pacific coast. There are

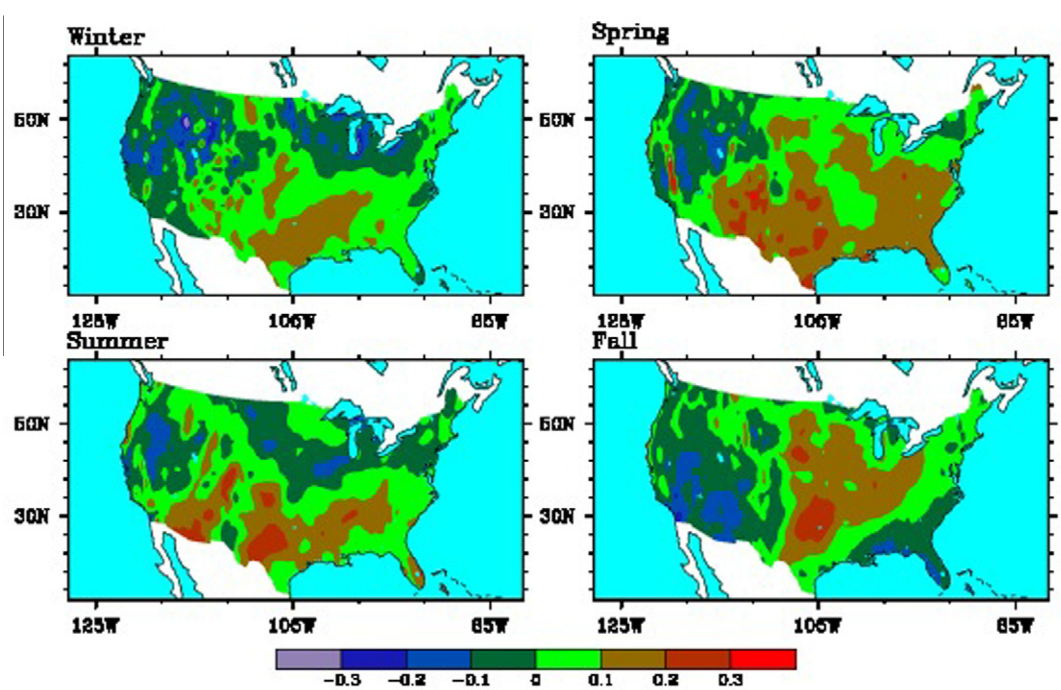

Fig. 4. Same as Fig. 1 except for surface wind speed (m/s).

Please cite this article in press as: Liu, Y., et al. Future U.S. wildfire potential trends projected using a dynamically downscaled climate change scenario. Forest Ecol. Manage. (2012), http://dx.doi.org/10.1016/j.foreco.2012.06.049

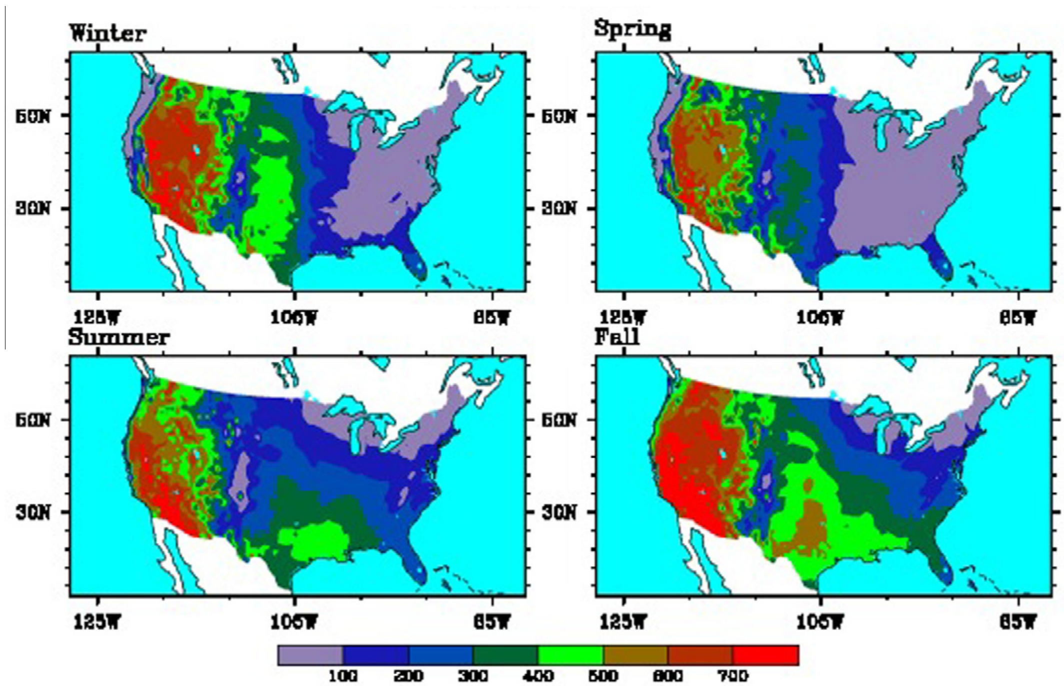

Fig. 5. Spatial patterns of present KBDI for the period of 1971–2000 in the continental U.S. The four panels are for winter, spring, summer, and autumn.

also large values in the Intermountain. KBDI values decrease rapidly towards the east and become less than 200 (low fire potential) in the Great Plains. This spatial pattern remains during other seasons but with some changes. The magnitude of KBDI in the western U.S. is slightly smaller in spring than winter. This trend however reverses in summer. Large KBDI values of over 300 (moderate fire potential) appear in the southern U.S. In autumn, KBDI values become larger in both the western and southern U.S., with the values of over 400 in the southern U.S. (high fire potential).

In the future (Fig. 6), KBDI values are expected to increase in the Southwest, Rockies, and the northern Great Plains by 100 with many areas over 200 in all four seasons. KBDI will increase in a large portion of the eastern U.S. by over 100 in summer and autumn with the largest increase of over 200 in the Appalachians in autumn. In contrast, KBDI will decrease west of the Rockies except a narrow Pacific coastal area, mainly in winter and spring.

3.2.2. Regional average

Regional averages of KBDI as well as meteorological elements were obtained to more quantitatively analyze and compare regional features, especially magnitude. The continental U.S. is divided into eight regions (Fig. S5) of Pacific South (PS) and Pacific North (PN) along the Pacific coast, Southwest (SW) and Northwest (NW) in the Rocky Mountains and the Intermountain, South Central (SC) and North Central (NC) in the central U.S., and Southeast (SE) and Northeast (NE) along the Atlantic coast. Averages were also obtained over the entire continental U.S. (US).

The results of regional KBDI are shown in Fig. 7. Present KBDI values in all regions except Southwest and Northwest first decrease from winter to spring, and then increase in summer and autumn. The values in Southwest and Northwest are larger in spring than in summer. The values are generally larger in the western than eastern U.S. regions. Fire potential, for example, are high in winter and summer, moderate in spring, and extreme in autumn in Pacific South, but only low in winter and spring and moderate in summer and autumn in Southeast.

Future KBDI values will increase in almost all seasons and regions. KBDI increases mostly by 100 or more in summer and autumn but by a much smaller amount in winter and spring. The temporal variations can be seen more clearly in the annual cycle of monthly KBDI (Fig. S6). Regional temperature increases by more than 2 °C in almost all seasons and regions (Fig. S7). The largest increase of almost 4 °C occurs in the summer; this warming would favor increases of KBDI. Regional seasonal precipitation (Fig. S8) mostly increases across all seasons, with the largest increase of more than 40 mm in winter and/or spring in Southeast and Northeast. This would favor decreases in KBDI. The projected overall increases in KBDI suggest that the future temperature change plays a more important role than precipitation change in fire potential trends.

Future KBDI is reduced by about 50 in winter and spring in Pacific South and Pacific North. This seemly disagrees with the corresponding temperature and precipitation changes. Temperature increases by about 2 °C, favoring an increase of KBDI. Precipitation changes differently, depending on season and region. Precipitation in Pacific South and Pacific North either changes little or increases in winter and spring, which is at least not in favor of a decrease in KBDI.

This apparent disagreement could be explained from the feature of the largest amount of rainfall in winter rather than a warm season in Pacific South and Pacific North. It can be derived from Eqs. (S1) and (S2) that daily KBDI incremental rate is negative (i.e., $dQ < 0$) when temperature $T < 6.9$ °C, or when $T > 6.9$ °C but daily rainfall (dP) is large enough to overcome the contribution from temperature. Winter rainfall is extremely large (about 500 mm) in Pacific South and Pacific North. Meanwhile, winter temperature is relatively low, about 10 and 5 °C in Pacific South and Pacific North, respectively. Thus, it is expected that daily KBDI incremental rate calculated using Eqs. (S1) and (S2) would be negative on a number of days in winter. However, final KBDI values, which are shown in Fig. 7, are those with an adjustment of $dQ = 0$ to those days when $T \leqslant 10$ °C; they therefore are higher than those calculated using Eqs. (S1) and (S2).

In the future, temperature will increase and thus the days on which an adjustment is needed should be reduced by a certain number. On the reduced number of days, instead of $dQ = 0$ at

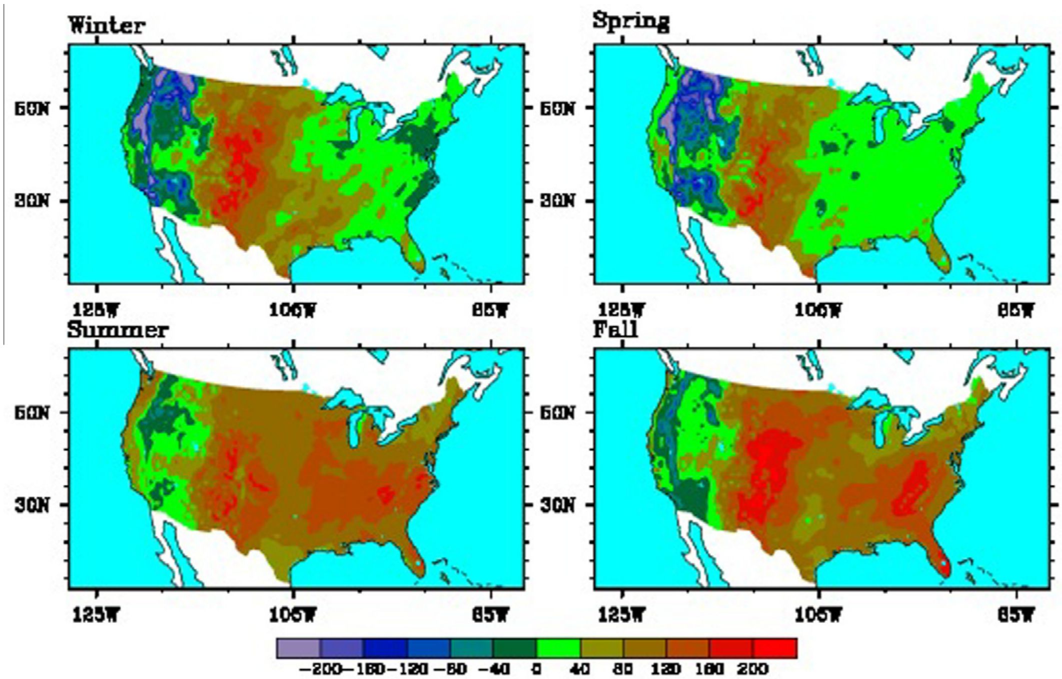

Fig. 6. Same as Fig. 5 except for changes in KBDI between 2041–2070 and 1971–2000.

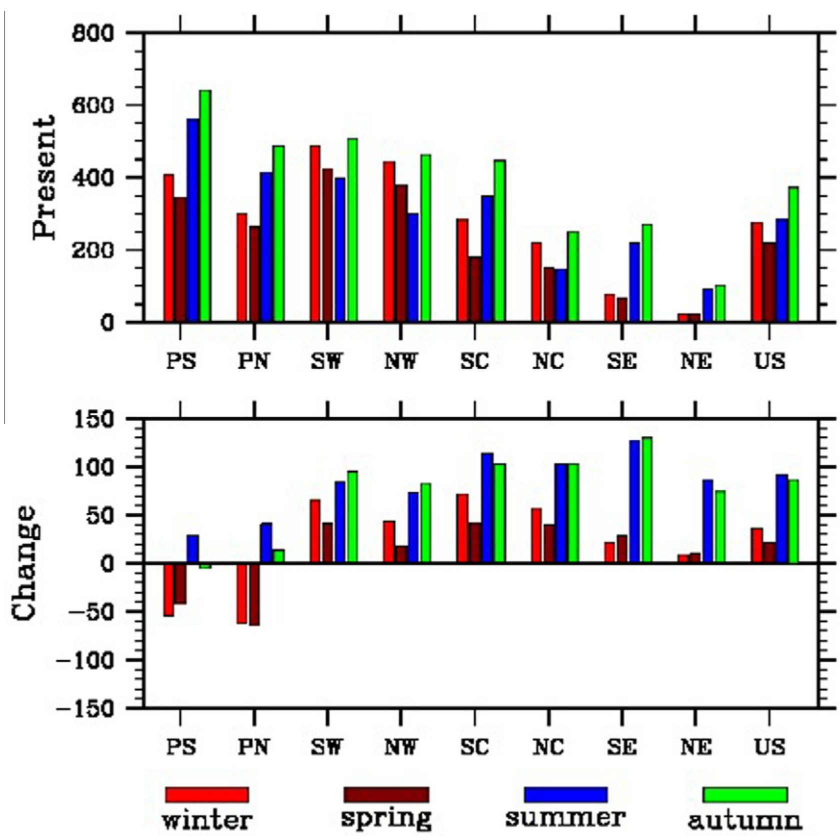

Fig. 7. Regional averages of seasonal KBDI. The top and bottom panels are for the present period of 1971–2000 and future change between 2041–2070 and 1971–2000. The regions indicated below each panel are Pacific South (PS), Pacific North (PN), Southwest (SW), Northwest (NW), South Central (SC), North Central (NC), Southeast (SE), Northeast (NE), as well as continental U.S. (US) (see Fig. S5 for geographic areas of these regions).

present, dQ would not be zero in future and it is more likely that $dQ < 0$ because of a large amount of winter rainfall. Thus, future winter KBDI values could be negative even with increased temperature and decreased precipitation. This also could happen in spring partially because spring KBDI values depend on antecedent winter values.

Table 1
KBDI values in Pacific South (PS) and Pacific North (PN). Calculated with and without an adjustment of $dQ = 0$ when $T \leqslant 10$ °C.

Region	Season	With adjustment		w/o adjustment	
		Present	Change	Present	Change
PS	Winter	406	−53	235	10
	Spring	345	−42	183	22
PN	Winter	298	−61	71	7
	Spring	261	−63	45	10

We conducted a calculation of KBDI but without an adjustment when $T \leqslant 10$ °C. The obtained KBDI values are no longer negative in winter and spring in Pacific South and Pacific North (Table 1). This therefore provides a proof for the above explanation.

Studies (e.g., Gillett et al., 2004; Flannigan et al., 2005; Balshi et al., 2008; Liu et al., 2010; Parisien et al., 2011) have indicated that future warming is a more important contributor to projected increasing fire potential than the change in precipitation. Fig. 8 compares KBDI results calculated with changes in both temperature and precipitation, temperature only, and precipitation only (without an adjustment when $T \leqslant 10$ °C). For the regions and seasons with noticeable KBDI increases (50 or more), the magnitude of KBDI change due to the change in temperature is much larger than that due to the change in precipitation. The latter is close to 30% of the former only at South Central during winter and fall and in Southeast during fall.

3.2.3. Variability and trends

Standard deviation (SD) was calculated for two types of KBDI time series in each region. One is a single series consisting of seasonal KBDI values changing first from winter to autumn and then from year 1 to year 30 of the present or future period. The resultant standard deviation measures inter-seasonal variability of seasonal KBDI. The result is shown in Fig. 9. The present standard deviation has large values over 120 in Pacific South and South Central, and a small value of less than 60 in Northeast. Other regions have the values in between. The U.S. has a value of about 75. The future standard deviation changes are different between the coastal and non-coastal regions. Standard deviation in the four coastal regions will increase by 25–50, but only by less than 10 or even decrease in the non-coastal regions.

The second type of KBDI time series has four sub-series, each of which consists of KBDI values for a single season (winter, spring, summer, or autumn) from year 1 to year 30 of the present or future period. The resultant standard deviation measures inter-annual variability of seasonal KBDI. The result is shown in Fig. 10. The standard deviation values in the non-coastal regions are generally larger at present, ranging between 90 and 110. However, they will mostly decrease in the future. In contrast, those in the coastal region are smaller at present, but likely will increase in future. The US has values between 40 and 60 at present; they will reduce in future by up to 20.

Fig. 11 shows time series of summer KBDI anomalies over the present and future 30-year periods. The values are expressed as

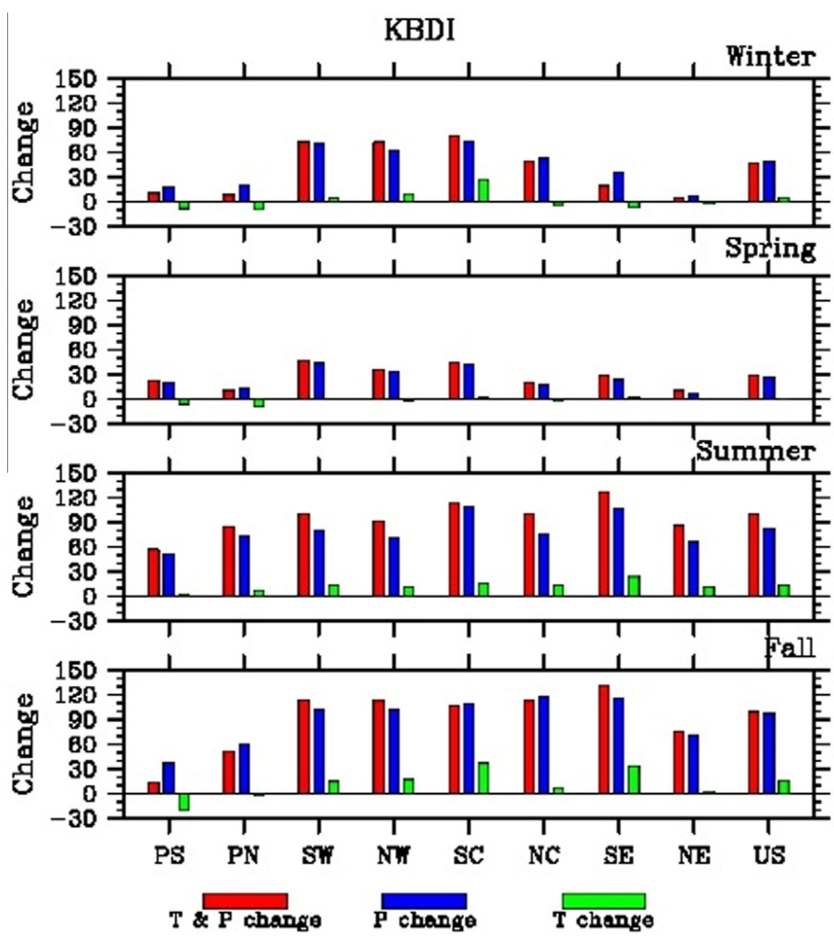

Fig. 8. Regional averages of KBDI in winter, spring, summer and autumn (from top to bottom). T&P change, P change, and T change represent KBDI change in response to the changes in both temperature and precipitation, temperature only, and precipitation only, respectively. The labels below each panel are regions (see Fig. S5 for the geographic areas of these regions).

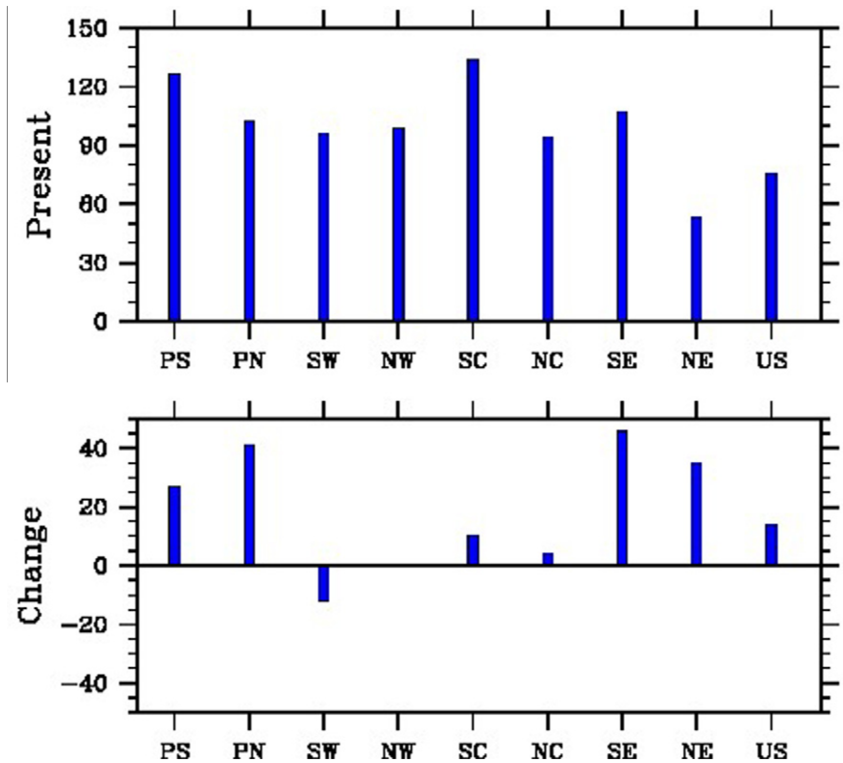

Fig. 9. Inter-seasonal KBDI variability. The bars are standard deviation of seasonal KBDI time series, which consists of KBDI values changing from winter to fall and from year 1 to 30. Top panel is KBDI values at present period of 1971–2000 and bottom one is the change between 2041–2070 and 1971–2000. The labels below each panel are regions (see Fig. S5 for the geographic areas of these regions).

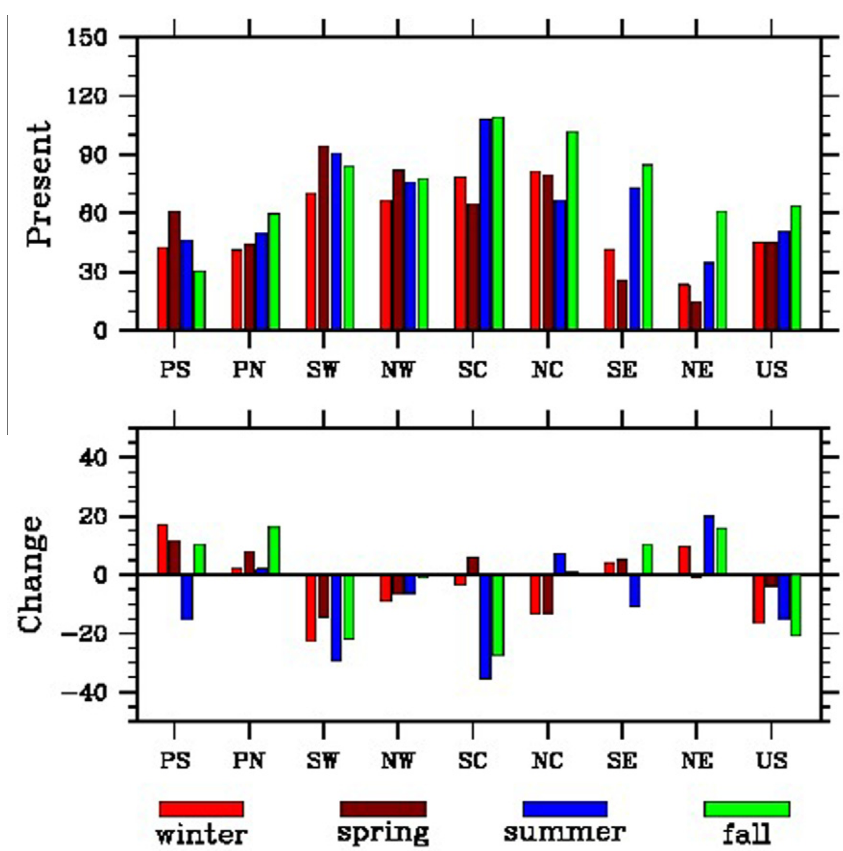

Fig. 10. Same as Fig. 9 except for inter-annual variability. The bars for are standard deviation values of four sub-series each consisting of one-season (winter, spring, summer, or autumn) KBDI values changing from year 1 to year 30 of the present or future period. The labels below each panel are regions (see Fig. S5 for the geographic areas of these regions).

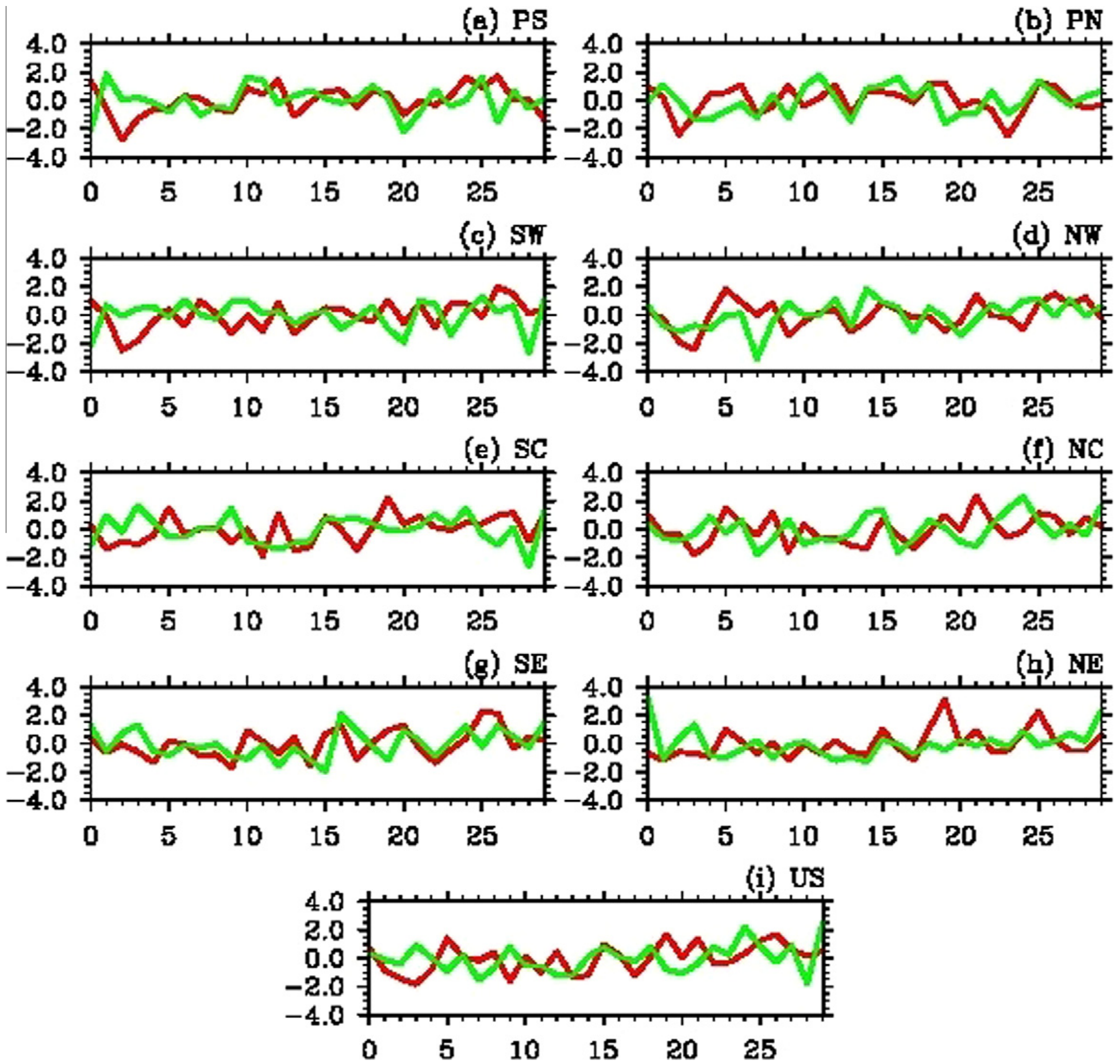

Fig. 11. Variations of summer KBDI. The red and green lines represent the present period of 1971–2000 and future period of 2041–2070. The nine panels are for averages at each region and the continental U.S. (see Fig. S5 for the geographic areas of these regions).

departures of individual summers from the average of all summers divided by standard deviation. KBDI values vary remarkably from 1 year to another, as indicated by multiple peaks (valleys) that occur mostly every 1–3 years for both present and future periods.

The trend of seasonal KBDI values in a region is measured by the slope of a linear line fitting the normalized KBDI time series. Note that the term trend here refers to a tendency over the present or future period of 30 years rather than a change from present to future period. A positive (negative) sign of slope indicates an increasing (decreasing) trend. The calculated slopes are listed in Table 2. Present slopes have a positive sign in all seasons and regions except three seasons in Pacific North and two seasons in Southeast, indicating overall increasing trends of KBDI over the period of 1971–2000. The magnitude is greater than 4.0 for all seasons in Southwest and summer and autumn in South Central. The US averages are greater than 2.0 in summer and autumn. The future slopes also show increasing trends, but much less noticeable than the present period. There are no seasons in any individual regions with a magnitude greater than 4.0 and no seasons in the U.S. averages with a magnitude greater than 2.0.

3.2.4. Local KBDI features

Fire potential changes at a local scale were analyzed using the southern U.S. (including South Central and Southeast) as an example. Strong impacts of climate and climate change have been recognized for this region (e.g., Heilman et al., 1998). The southern U.S. is divided into six eco-regions (Fig. S9): Atlantic Coastal Plain (AC), Piedmont (PI), Appalachian–Cumberland (AP), Mississippi Alluvial Valley (MI), Gulf Coastal Plain (GC), and Mid-South (MS). Present KBDI values are usually small in winter and spring and large in summer and autumn in all eco-regions (Fig. 12). Present summer and autumn KBDI values are around 200 (upper KBDI range for low fire potential or lower range for moderate fire potential) in the three eastern eco-regions, and future values change to about 350–400 (upper KBDI range for moderate fire potential or lower range for high fire potential). Meanwhile, present summer and autumn KBDI values are around 400 (upper KBDI range for moderate fire potential or lower range for high fire potential) in the three western eco-regions, and future values change to about 500 (middle KBDI range for high fire potential). For the entire South, summer and autumn fire potential changes from moderate at present to high fire potential in future.

Please cite this article in press as: Liu, Y., et al. Future U.S. wildfire potential trends projected using a dynamically downscaled climate change scenario. Forest Ecol. Manage. (2012), http://dx.doi.org/10.1016/j.foreco.2012.06.049

Table 2
Slopes of fitting linear lines of KBDI variation curves over 30-year periods.

Region	Present				Future			
	Winter	Spring	Summer	Autumn	Winter	Spring	Summer	Autumn
PS	0.45	2.25	2.41	0.96	82.09	−1.60	−0.16	0.04
PN	−0.85	−0.30	0.63	−0.13	−1.10	−1.88	1.04	1.48
SW	4.36	4.68	4.67	4.16	−1.74	−1.51	−0.85	−0.28
NW	2.23	2.75	2.06	2.48	2.07	1.51	2.47	3.07
SC	2.58	0.73	4.99	4.66	−3.87	−1.38	0.99	−0.25
NC	2.58	1.90	1.18	2.79	−0.06	−0.59	2.00	3.42
SE	−0.40	−0.16	2.96	3.55	−1.96	0.72	1.55	1.94
NE	0.80	0.21	1.67	2.65	−1.42	0.08	2.45	1.07
US	1.95	1.64	2.82	3.11	−1.37	−0.71	1.22	1.30

The length of a fire season, measured by the number of the months with high or extreme fire potential level, will increase by 1–3 months (Fig. 13).

3.3. Sensitivity analyses

3.3.1. mFFWI

Fig. 14 shows spatial pattern of present seasonal mFFWI. Present mFFWI values are large in the Pacific coast, Intermountain, and southern Great Plains, while small in the Rocky Mountains. The magnitude increases from winter to summer, and then decreases. This spatial pattern is generally similar to that of KBDI. However, the magnitude of the large mFFWI values in the western U.S. decreases rapidly toward the north. This is caused by the higher relative humidity and smaller wind speed in the northwestern as compared to the southwestern U.S.

Future mFFWI values will increase in most regions except the Pacific coast and Intermountain (Fig. 15). The largest increases are found in Southwest and Northwest in winter and spring, and expand to South Central as well as Southeast in summer and autumn. This pattern is similar to that of KBDI change. But again, the future mFFWI change is more remarkable in the southern portions except for autumn. In addition, no pronounced increase in mFFWI value is in the eastern U.S.

3.3.2. GCM–RCM combinations

Fig. 16 shows KBDIs calculated using the seasonal averages of temperature and precipitation over Central Plains or Deep South and present or future simulation period (see Supplementary material). A comparison of KBDI calculation for HadCM3–HRM3 using the average and daily (shown in parentheses) temperature and precipitation indicates that the present KBDIs in Central Plains

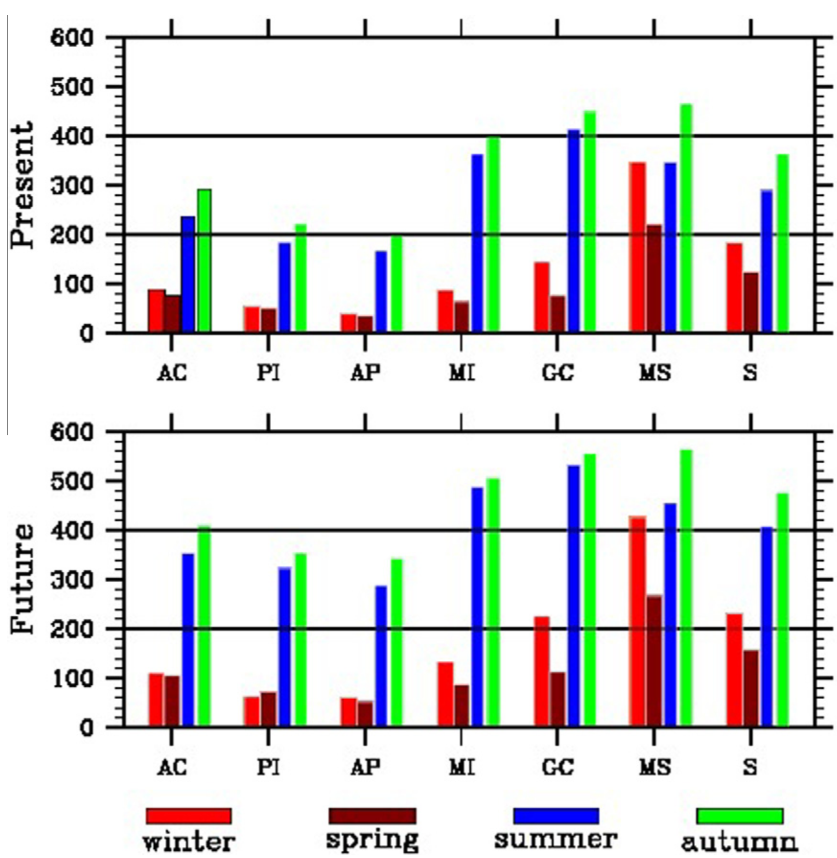

Fig. 12. KBDI in the southern U.S. eco-regions. The top and bottom panels are for the present period of 1971–2000 and future period of 2041–2070. The regions indiated below each panel are Atlantic Coast (AP), Piedmont (PI), Appalachian (AP), Mississippi (MI), Gulf Coast (GC), Mid-South (MS), and entire souther U.S. (US) (see Fig. S9 for georgraphic areas of these regions).

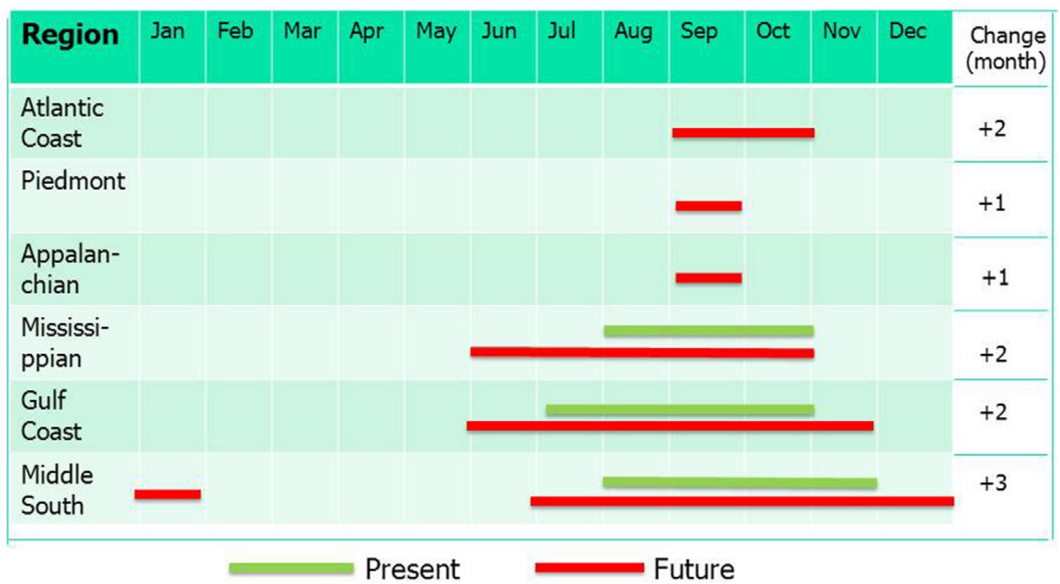

Fig. 13. Fire season lengths. The rows are the southern U.S. eco-regions and columns are months of a year. The numbers in the right-hand table are future change in the number of months for a fire season (high or extreme fire potential) between 2041–2070 and 1971–2000.

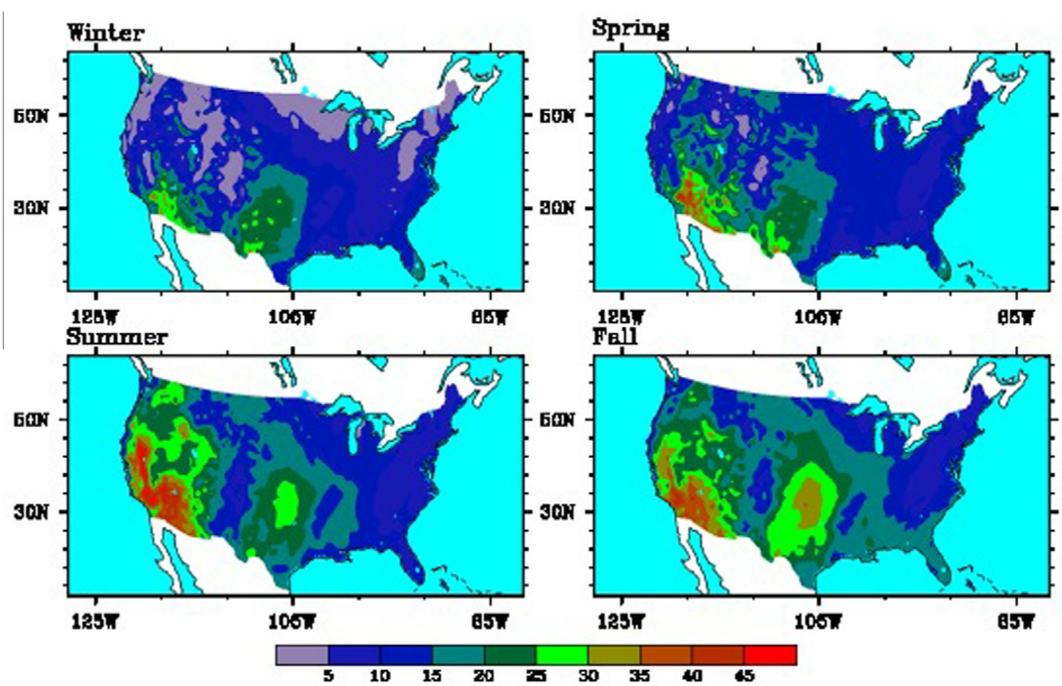

Fig. 14. Spatial patterns of present modified Fosberg Fire Weather Index for the period of 1971–2000 in the continental U.S. The four panels are for winter, spring, summer, and autumn.

are 248 (250) in winter and 283 (246) in summer, and the future KBDI changes are 85 (65) in winter and 102 (109) in summer. The corresponding values in Deep South are 183 (180) in winter and 277 (281) in summer for the present KBDIs, and 33 (92) in winter and 138 (121) in summer for future changes. Thus, KBDI values are comparable between the two climate datasets except future winter change in Deep South.

Future KBDI changes for all model combinations are about the same between winter and summer in Central Plains. In comparison with HadCM3–HRM3 whose changes are about 100, the changes are about the same CCSM–MM5I and GFDL–RSM, 50% larger with CCSM–WRFG and GFDL–WRFG, and 100% larger with CGCM3–CRCM and CGCM3–RCM3. The extreme changes come up with GFDL–HRM3 (increasing by 300–350) and CGCM3–WRFG (decreasing by 60–80). It seems that the smaller KBDI increase for HadCM3–HRM3, larger increase for GFDL–HRM3 and decrease for CGCM3–WRFG are mainly due to no rainfall decrease, large increasing temperature and decreasing rainfall, and increasing rainfall, respectively (Figs. S10 and S11).

In Deep South, the magnitude of KBDI increases is the same between winter and summer for four model combinations, but about doubled in summer for six combinations including HadCM3–HRM3. The changes for other combinations, ranging between about 100 and 300, are much larger than those for HadCM3–HRM3, which has a small increasing in contrast to decreasing rainfall for other model combinations.

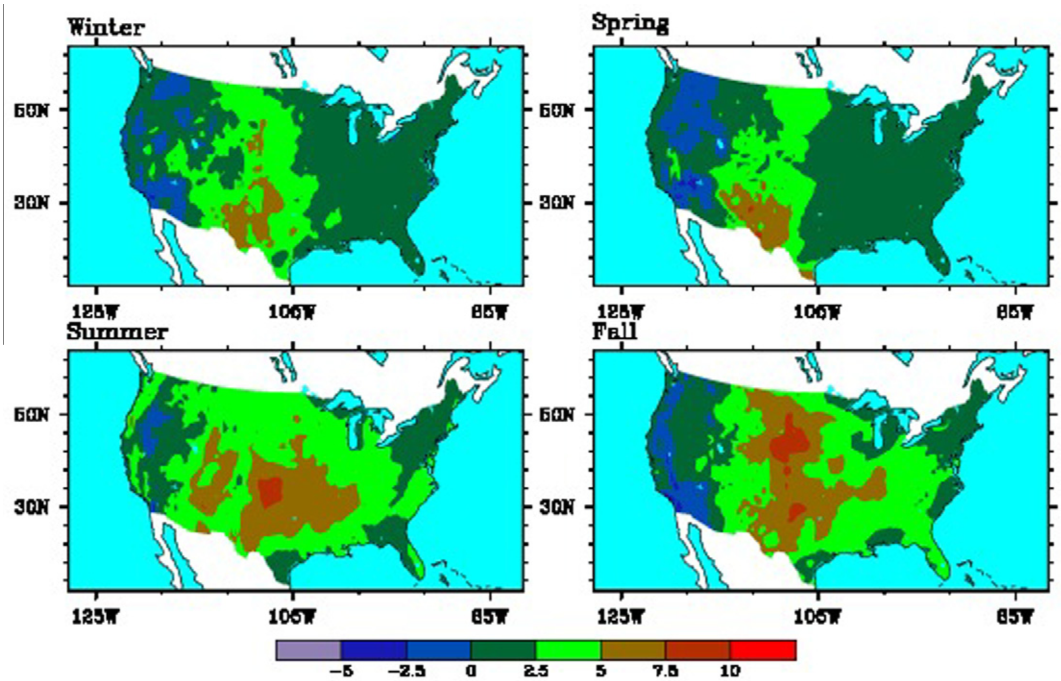

Fig. 15. Same as Fig. 14 except for the change between 2041–2070 and 1971–2000.

4. Discussion

4.1. KBDI calculated using global and regional climate model predictions

KBDI has been analyzed in this study for the continental U.S., which is a continuation of a global KBDI study (Liu et al., 2010). Future climate projections used in both studies were projected by HadCM3; the format of the projections used this study is the dynamical downscaling of the projections using the HRM3 regional climate model (Mearns et al., 2009). Besides the more detailed distributions due to higher spatial resolution with the downscaling, a major difference obtained in this study is the locations of major future fire potential increases. In the earlier study future KBDI increased mainly in the Midwest and central U.S., but in this study the Southwest and Rocky Mountains show more pronounced increases. The westward shift of the locations is due to the differences in the projected climate change between the global and regional climate models (Figs. S12 and S13). Both models project overall warming, but the region with largest magnitude moves from the central U.S. in HadCM3 to the Southwest and Rocky Mountains in HRM3. There are even more pronounced differences in the precipitation projections. Precipitation decreases mainly in the Northwest and central U.S. in the HadCM3 projection; the Southwest turns drier while the central U.S. as well as most parts of the eastern U.S. become wetter in the HRM3 downscaling. The differences in both temperature and precipitation contribute to the differences in KBDI spatial patterns between the two studies.

4.2. Future fire potential increases

The IPCC raised the possibility that changes in extreme weather and climate events due to greenhouse effects would increase the risk of wildfire (IPCC, 2007). This study indicates that fire potential is expected to increase in most of the continental U.S., which therefore provides an evidence for the IPCC's speculation. This study projects the large overall fire potential increases across all seasons in the western U.S., especially in the Southwest and Rocky Mountains. This agrees with many previous predictions for this region (e.g., Bachelet et al., 2001a, 2001b; Lenihan et al., 2003; Brown et al., 2004; Liu et al., 2005; Westerling et al., 2006; Spracklen et al., 2009; Rogers et al., 2011). Spracklen et al. (2009) projected an increase in burned area from late spring to early autumn by more than 100% in the Rocky Mountains and about 50% in the Pacific coast by the mid-21st century. Our study also predicts the largest fire potential increase in the Rocky Mountains and moderate increases in a narrow area along the Pacific coast. A difference between the two studies is in the Intermountain where a decrease is projected in this study but little change in Spracklen et al. (2009). While most previous studies have focused on the western U.S., this study investigates the continental U.S. with a detailed description for the southern U.S. and finds that fire potential will increase by one level in summer and autumn in most southern eco-regions.

4.3. Fire seasons

It has been found in previous studies that future fire seasons will become longer in many regions (e.g. Flannigan et al., 2009a, 2009b). This study investigates fire seasons by examining the change in future number of the months with KBDI reaching a certain level. There is a potential issue with this approach. As seen in Fig. 7 or Fig. S6, the KBDI peaks occur in autumn, but actual fire seasons occur in spring or summer in most regions (though parts of the southeastern U.S. experience both a spring and autumn fire season). Thus, the time spans are often different between a fire season defined here and an actual fire season. The issue of later time for KBDI peak occurrence was recognized in the original KBDI work (Keetch and Byram, 1968). One of the reasons is that KBDI changes exponentially in response to temperature but linearly to precipitation. In summer and autumn, KBDI keeps increasing with accumulated positive contribution of high temperature, which outweighs the adverse contribution from large precipitation.

4.4. Variability

This study has indicated pronounced increases in seasonal variability and slight increases in inter-annual variability in future fire potential in the coastal regions. Seasonal variability is a factor

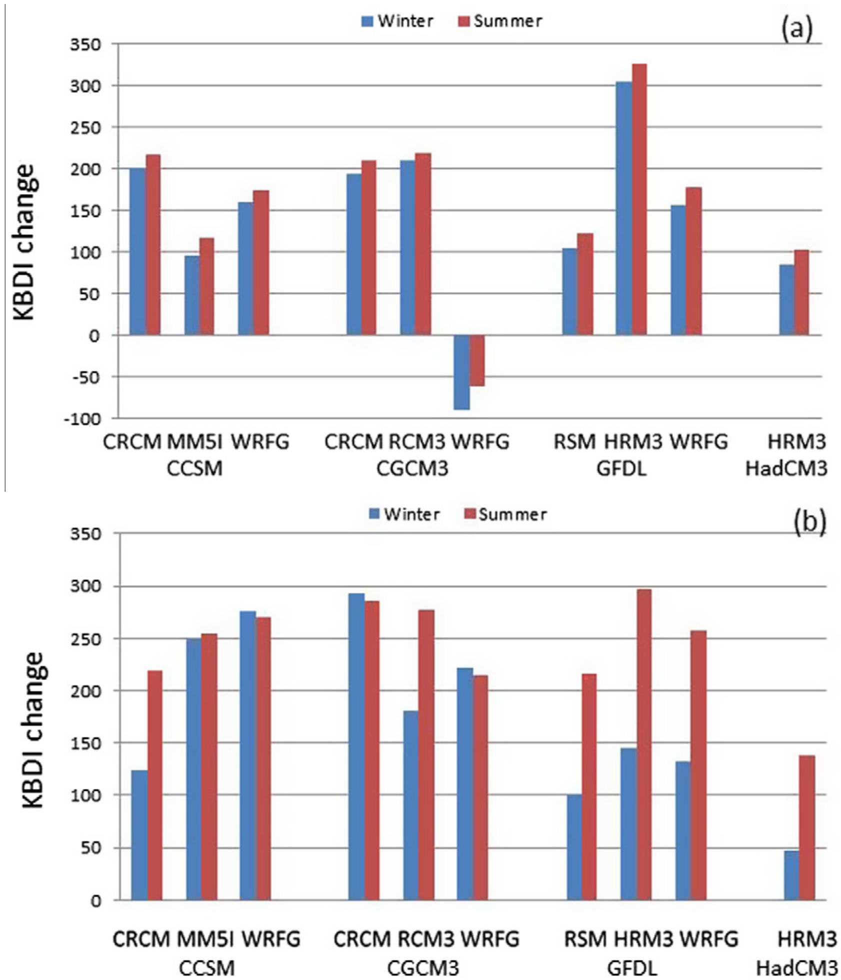

Fig. 16. Average future winter (blue) and summer (red) KBDI changes in Central Plains (a) and Deep South (b) regions. The labels below each panel are regional climate models (upper line) and the driving global climate models (bottom line) (see context for full names of the models).

determining predictability of fire season and is often related to atmospheric anomalies such as droughts. The increased variability means increased difficulty in seasonal prediction. Inter-annual variability of U.S. fire potential is often related to Pacific Ocean surface temperature anomalies and their remote connections with atmospheric conditions in the U.S. The increased inter-annual variability means increased uncertainty in annual fire planning. The impacts of the variability on seasonal prediction and annual planning, however, are minimal in the mountain and central regions. The uncertainty in annual fire planning is even expected to be reduced in some regions because of the reduced inter-annual variability. This study shows generally increasing trends of KBDI over the present period, indicating that the impacts of global warming on fire might already have been happening, as suggested for the western U.S. (Westerling et al., 2006).

4.5. Uncertainties

The difference with mFFWI indicates that, without considering the roles of relative humidity and wind speed, fire potential measured using KBDI would be over-estimated for present and future periods in the northern U.S., mainly the northern Rocky Mountains. In addition, as pointed in Liu et al. (2010), the exact functional form of the relationship between precipitation and vegetation used in the KBDI may not be valid for annual rainfall amounts that differ significantly from those of the southeastern U.S. where the index was developed, although KBDI is still a viable means of assessing the potential impacts of a changing climate on fire potential by focusing on the relative changes in KBDI produced by changes in temperature and precipitation. Of more concern is that vegetation itself will change as a result of climate change (Hansen et al., 2001) and it is not clear how well future precipitation can be used as a surrogate for future fuel conditions.

The NARCCAP climate change downscaling used only for the IPCC SRES A2 emission scenario. It was indicated in the global KBDI analysis (Liu et al., 2010) that A1 and B2 are extremely large and small emission cases, respectively, while A2 and B1 are moderate ones. Thus, it is expected that future wildfire potential using future climate change projections for the A1 and B2 emission scenarios would increase more and less noticeable, respectively, than the results obtained from this study.

5. Conclusions

Future potential wildfire trends in the continental U.S. have been projected using fire weather indices, mainly KBDI, calculated based on the dynamically downscaled climate projections. It can be concluded that fire potential is expected to increase overall in the continental U.S. The specific findings from this study include:

a. Fire potential indicated by KBDI is expected to increase in the Southwest, Rocky Mountains, northern Great Plains, Southeast, and Pacific coast. Future change in temperature is a major contributor.

b. Most pronounced increase occurs during summer and autumn. Fire season could become a few months longer in the South.
c. The magnitude of future fire potential increase will be reduced in the northwestern U.S. due to the impacts of future changes in humidity and wind.
d. The future KBDI increases in the central Plains and the South projected using the HadCM3–HRM3 climate change scenario are smaller than those projected using the climate change scenarios from most of other NARCCAP model combinations. The projected future climate is wetter in HadCM3–HRM3 than other model combinations.
e. Fire potential has been increasing across the continental U.S. in recent decades. Larger inter-seasonal and inter-annual variability in fire potential is expected in the future in the Pacific and Atlantic coasts.

The increased future fire potential and longer fire seasons mean increased possibility for more intense wildfire activity and therefore increases in human fatalities and property loss. This in turn means increased demand for resources for disaster prevention and recovery. More intense fire activity also means more emissions of carbon and particles and therefore more severe consequences related to the adverse environmental effects of wildfires.

Further research is needed to improve projections of future trends and impacts of wildfires in the continental U.S. First, there is a need to conduct sensitivity studies to quantify the uncertainties related to selections of particular fire weather indices, global and regional climate model projections, and CO_2 emission scenario, as described in Section 4. Second, there is a need to project actual fire properties such as occurrence, severity, burned area, and seasonality. One challenge is that actual fire behavior is determined not only by weather and climate, but also human activity and fuel conditions. Fuel conditions would change as well under a changing climate. Another needed area of research is the environmental impacts of potentially increased fire activities, including the air quality impacts and the atmospheric feedback of greater emissions of particulate as well as gaseous carbon.

Acknowledgements

This study was supported by the U.S. Joint Fire Science Program under Agreement No. JFSP 11172. The meteorological data were obtained from the North America Regional Climate Change Assessment Program (NARCCAP).

Appendix A. Supplementary material

Supplementary data associated with this article can be found, in the online version, at http://dx.doi.org/10.1016/j.foreco.2012.06.049.

References

Ackerman, A.S., Toon, O.B., Stevens, D.E., Heymsfield, A.J., Ramanathan, V., Welton, E.J., 2000. Reduction of tropical cloudiness by soot. Science 288, 1042–1047.
Amiro, B.D., Stocks, B.J., Alexander, M.E., Flannigan, M.D., Wotton, B.M., 2001. Fire, climate change, carbon and fuel management in the Canadian boreal forest. Int. J. Wildland Fire 10, 405–413.
AP (Associated Press), 2009. 108 Killed in Deadliest-Ever Australian Wildfires. <http://www.ap.org> (08.02.09).
Bachelet, D., Lenihan, J.M., Daly, C., Neilson, R.P., Ojima, D.S., Parton, W.J., 2001a. MC1: A Dynamic Vegetation Model for Estimating the Distribution of Vegetation and Associated Carbon, Nutrients, and Water – Technical Documentation. Version 1.0. General Technical Report PNW-GTR-508. Portland, OR: U.S. Department of Agriculture, Forest Service, Pacific Northwest Research Station.
Bachelet, D., Neilson, R.P., Lenihan, J.M., Drapek, R.J., 2001b. Climate change effects on vegetation distribution and carbon budget in the United States. Ecosystems 4, 164–185.
Balshi, M.S., McGuire, A.D., Duffy, P., Flannigan, M.D., Walsh, J., Melillo, J., 2008. Assessing the response of area burned to changing climate in western boreal North America using a Multivariate Adaptive Regression Splines (MARS) approach. Global Change Biol. 15, 578–600. http://dx.doi.org/10.1111/j.1365-2486.2008.01679.x.
Brown, T.J., Hall, B.L., Westerling, A.L., 2004. The impact of twenty-first century climate change on wildland fire danger in the western United States: an applications perspective. Clim. Change 62, 365–388.
Charlson, R.J., Schwartz, S.E., Hales, J.M., Cess, R.D., Coakley Jr., J.A., Hansen, J.E., Hoffman, D.J., 1992. Climate forcing by anthropogenic sulfate aerosols. Science 255, 423–430.
Chu, P.-S., Yan, W.P., Fujioka, F., 2002. Fire–climate relationships and long-lead seasonal wildfire prediction for Hawaii. Int. J. Wildland Fire 11, 25–31.
Cochrane, M.A., 2003. Fire science for rainforests. Nature 421, 913–919.
Flannigan, M.D., Harrington, J.B., 1988. A study of the relation of meteorological variables to monthly provincial area burned by wildfire in Canada 1953–80. J. Appl. Meteorol. 27, 441–452.
Flannigan, M., Campbell, I., Wotton, M., Carcaillet, C., Richard, P., Bergeron, Y., 2001. Future fire in Canada's boreal forest: paleoecology results and general circulation model-regional climate model simulations. Canadian J Forest Res 31, 854–864.
Flannigan, M.D., Logan, K.A., Amiro, B.D., Skinner, W.R., Stocks, B.J., 2005. Future area burned in Canada. Clim. Change 72, 1–16.
Flannigan, M.D., Stocks, B., Turetsky, M., Wotton, W., 2009a. Impacts of climate change on fire activity and fire management in the circumboreal forest. Global Change Biol. 15, 549–560.
Flannigan, M.D., Krawchuk, M.A., de Groot, W.J., Wotton, B.M., Gowman, L.M., 2009b. Implications of changing climate for global wildland fire. Int. J. Wildland Fire 18, 483–507.
Foley, J., Kucharik, C., Polzin, D., 2005. Integrated Biosphere Simulator Model (IBIS), Version 2.5. Model product. Available on-line [http://daac. ornl. gov] from Oak Ridge National Laboratory Distributed Active Archive Center, Oak Ridge, Tennessee, USA http://dx.doi.org/10.3334/ORNLPAAC/808.
Forster, P., Ramaswamy, V., Artaxo, P., Berntsen, T., Betts, R., Fahey, D.W., Haywood, J., Lean, J., Lowe, D.C., Myhre, G., Nganga, J., Prinn, R., Raga, G., Schulz, M., Van Dorland, R., 2007. Changes in atmospheric constituents and in radiative forcing. In: Solomon, S., Qin, D., Manning, M., Chen, Z., Marquis, M., Averyt, K.B., Tignor, M., Miller, H.L. (Eds.), Climate Change 2007: The Physical Science Basis. Contribution of Working Group I to the Fourth Assessment Report of the Intergovernmental Panel on Climate Change. Cambridge University Press, Cambridge, United Kingdom and New York, NY, USA.
Friend, A.D., Stevens, A.K., Knox, R.G., Cannell, M.G.R., 1995. A process-based terrestrial biosphere model of ecosystem dynamics (Hybrid v3.0). Ecol. Model. 95, 249–287.
Giglio, L., Randerson, J.T., van der Werf, G.R., Kasibhatla, P.S., Collatz1, G.J., Morton, D.C., DeFries, R.S., 2010. Assessing variability and long-term trends in burned area by merging multiple satellite fire products. Biogeosciences 7, 1171–1186.
Gillett, N.P., Weaver, A.J., Zwiers, F.W., Flannigan, M.D., 2004. Detecting the effect of climate change on Canadian forest fires. Geophys. Res. Lett. 31, L18211. http://dx.doi.org/10.1029/2004GL020876.
Goldhammer, J.G., Price, C., 1998. Potential impacts of climate change on fire regimes in the tropics based on Magicc and a GISS GCM-derived lightning model. Clim. Change 39, 273–296.
Groisman, P.Y., Sherstyukov, B.G., Razuvaev, V.N., Knight, R.W., Enloe, J.G., Stroumentova, N.S., Whitfield, P.H., Førland, E., Hannsen-Bauer, I., Tuomenvirta, H., Aleksandersson, H., Mescherskaya, A.V., Karl, T.R., 2007. Potential forest fire danger over Northern Eurasia: changes during the 20th century. Global Planet. Change 56, 371–386.
Hansen, A.J., Neilson, R.P., Dale, V., Flather, C., Iverson, L., Currie, D.J., Shafer, S., Cook, R., Bartlein, P.J., 2001. Global change in forests: responses of species, communities, and biomes. BioScience 51, 765–779.
Hansen J., Nazarenko L., 2004. Soot climate forcing via snow and ice albedos. Proc. Natl. Acad. Sci. 101.
Heilman, W.E., Potter, B.E., Zerbe, J.I., 1998. Regional climate change in the southern United States: the implications for wildfire occurrence. In: Mickler, R.A., Fox, S. (Eds.), The Productivity and Sustainability of Southern Forest Ecosystems in a Changing Environment. Springer-Verlag, New York, NY, pp. 683–699. fpl.fs.fed.us/documnts/pdf1998/heilm98a.pdf.
IPCC (Intergovernmental Panel on Climate Change), 2007. Climate Change 2007.
Keetch, J.J., Byram, G.M., 1968. A Drought Index for Forest Fire Control. USDA Forest Service, Southeast Forest Experiment Station Research Paper SE-38. Asheville, NC, 32 pp.
Krawchuk, M.A., Moritz, M.A., Parisien, M.A., van Dorn, J., Hayhoe, K., 2009. Global pyrogeography: macro-scaled statistical models for understanding the current and future distribution of fire. PLoS ONE 4, e5102.
Langmann, B., Duncan, B., Christiane, T., Trentmannd, J., van der Werf, G.R., 2009. Vegetation fire emissions and their impact on air pollution and climate. Atmos. Environ. 43, 107–116.
Lenihan, J.M., Drapek, R.J., Bachelet, D., Neilson, R.P., 2003. Climate change effects on vegetation distribution and carbon budget in the U.S. Ecol. Appl. 13 (6), 1667–1681.

Levis, S.G., Bonan, B., Vertenstein, M., Oleson, K.W., 2004. The Community Land Model's Dynamic Global Vegetation Model (CLM-DGVM): Technical Description and User's Guide, NCAR Tech. Note TN-459+IA, NCAR, Boulder, Colorado, 50 pp.

Liu, Y.-Q., 2005a. Enhancement of the 1988 Northern U.S. drought due to wildfires. Geophys. Res. Lett. 32(10), L10806. http://dx.doi.org/10.1029/2005GL022411.

Liu, Y.-Q., 2005b. Atmospheric response and feedback to radiative forcing from biomass burning in tropical South America. Agric. Forest Meteorol. 133, 40–57.

Liu, Y.-Q., Stanturf, J., Tian, H., Qu, J., 2005a. CO_2 emissions from wildfires in the U.S.: present status and future trends. In: The Third USDA Greenhouse Gas Symposium, Baltimore, ND, March 21–24, pp. 1–12. www.oregon.gov/ODF/BOARD/docs/FFAC_LiuYong_CO2.pdf?ga=t.

Liu, Y.-Q., Stanturf, J., Goodrick, S., 2010. Trends in global wildfire potential in a changing climate. Forest Ecol. Manage. 259, 378–1127. http://dx.doi.org/10.1016/j.foreco.2009.09.002.

Mearns, L.O., 2012, Climate change results, 2012 Users' Meeting of the North American Regional Climate Change Assessment Program, Boulder, CO, April 10–11, 2012.

Mearns, L.O., Gutowski, W.J., Jones, R., Leung, L.-Y., McGinnis, S., Nunes, A.M.B., Qian, Y., 2009. A regional climate change assessment program for North America. EOS 90(36), 311–312.

Melton, M., 1989. Keetch–Byram Drought Index: a guide to fire conditions and suppression problems. Fire Manage. Notes 50 (4), 30–34.

Nakicenovic, N. et al., 2000. Special Report on Emissions Scenarios: A Special Report of Working Group III of the Intergovernmental Panel on Climate Change. Cambridge University Press, Cambridge, UK, 599pp.

Page, S.E., Siegert, F., Rieley, J.O., Boehm, H.-D.V., Jaya, A., Limin, S., 2002. The amount of carbon released from peat and forest fires in Indonesia during 1977. Nature 420, 61–65.

Parisien, M.-A., Parks, S.A., Krawchuk, M.A., Flannigan, M.D., Bowman, L.M., Moritz, M.A., 2011. Scale-dependent controls on the area burned in the boreal forest of Canada, 1980–2005. Ecol. Appl. 21, 789–805.

Pechony, O., Shindell, D.T., 2010. Driving forces of global wildfires over the past millennium and the forthcoming century. PNAS 107 (45), 19167–19170.

Piñol, J., Terradas, J., Lloret, F., 1998. Climate warming, wildfire hazard, and wildfire occurrence in coastal eastern Spain. Clim. Change 38, 345–357.

Pyne, S., Andrews, P.L., Laven, R.D., 1996. Introduction to Wildland Fire. John Wiley & Sons, Inc., 769pp.

Randerson, J.T., Liu, H., Flanner, M.G., Chambers, S.D., Jin, Y., Hess. P.G., Pfister, G., Mack, M.C., Treseder, K.K., Welp, L.R., Chapin, F.S., Harden, J.W., Goulden, M.L., Lyons, E., Neff, J.C., Schuur, E.A., Zender, C.S., (2006. The impact of boreal forest fire on climate warming. Science 314(5802), 1130–1132.

Reinhard, M., Rebetez, M., Schlaepfer, R., 2005. Recent climate change: rethinking drought in the context of forest fire research in Ticino, south of Switzerland. Theor. Appl. Climatol. 82, 17–25.

Riebau, A.R., Fox, D., 2001. The new smoke management. Int. J. Wildland Fire 10, 415–427.

Rogers, B.M., Neilson, R.P., Drapek, R., Lenihan, J.M., Wells, J.R., Bachelet, D., Law, B.E., 2011, Impacts of climate change on fire regimes and carbon stocks of the U.S. Pacific Northwest. J. Geophys. Res. 116, G03037. http://dx.doi.org/10.1029/2011JG001695.

Scholze, M., Knorr, W., Arnell, N.W., Prentice, I.C., 2006. A climate-change risk analysis for world ecosystems. Proc. Natl. Acad. Sci. USA 103, 13116–13120. http://dx.doi.org/10.1073/PNAS.0601816103.

Sitch, S., Smith, B., Prentice, I.C., Arneth, A., Bondeau, A., Cramer, W., Kaplan, J.O., Levis, S., Lucht, W., Sykes, M.T., Thonicke, K., Venevsky, S., 2003. Evaluation of ecosystem dynamics, plant geography and terrestrial carbon cycling in the LPJ Dynamic Global Vegetation Model. Global Change Biol. 9, 161–185.

Snyder, R.L., Spano, D., Duce, P., Baldocchi, D., Xu, L., Paw, U.K.T., 2006. A fuel dryness index for grassland fire-danger assessment. Agric. Forest Meteorol. 139, 1–11.

Spracklen, D.V., Mickley, L.J., Logan, J.A., Hudman, R.C., Yevich, R., Flanning, M.D., Westerling, A.L., 2009. Impacts of climate change from 2000 to 2050 on wildfire activity and carbonaceous aerosol concentrations in the western United States. J. Geophys. Res. 114, D20301. http://dx.doi.org/10.1029/2008JD010966.

Stocks, B.J., Mason, J.A., Todd, J.B., Bosch, E.M., Wotton, B.M., Amiro, B.D., Flannigan, M.D., Hirsch, K.G., Logan, K.A., Martell, D.L., Skinner, W.R., 2003. Large forest fires in Canada, 1959–1997. J. Geophys. Res. 108, 8149. http://dx.doi.org/10.1029/2001JD000484.

Stohl, A., Andrews, E., Burkhart, J.F., Forster, C., Kowal, D., Lunder, C., Mefford, T., Ogren, J.A., Sharma, S., Spichtinger, N., Stebel, K., Stone, R., Ström, J., Tørseth, K., Wehrli, C., 2006. Pan-Arctic enhancements of light absorbing aerosol concentrations due to North American boreal forest fires during summer 2004. J. Geophys. Res. 111, D22214. http://dx.doi.org/10.1029/2006JD007216.

Tacconi, L., Moore, P.F., Kaimowitz, D., 2007. Fires in tropical forests – what is really the problem? Lessons from Indonesia. Mitigat. Adapt. Strat. Global Change 12, 55–66.

Tian, H., Chen, G., Liu, M., Zhang, C., Sun, G., Lu, C., Xu, X., Ren, W., Pan, S., Chappelka, A., 2010. Model estimates of net primary productivity, evapotranspiration, and water use efficiency in the terrestrial ecosystems of the southern United States. Forest Ecol. Manage. 259, 1311–1327. http://dx.doi.org/10.1016/j.foreco.2009.10.009.

UNFAO (Food and Agriculture Organization of United Nations), 2001, Global Forest Fire Assessment 1990–2000 (Forest Resources Assessment – WP 55).

USFA (U.S. Forest Service), 2005. Fire Statistics. <http://www.usfa.fema.gov/wildfire/>.

van der Werf, G.R., Randerson, J.T., Giglio, L., Collatz, G.J., Mu, M., Kasibhatla, P.S., Morton, D.C., DeFries, R.S., Jin, Y., van Leeuwen, T.T., 2010. Global fire emissions and the contribution of deforestation, savanna, forest, agricultural, and peat fires (1997–2009). Atmos. Chem. Phys. Discuss. 10, 16153–16230. http://dx.doi.org/10.5194/acpd-10-16153-2010.

Van Wagner, C.E., 1987. The Development and Structure of the Canadian Forest Fire Weather Index System. Forestry Technical Report No. 35. Canadian Forest Service, Ottawa, Canada.

Westerling, A.L., Hidalgo, H.G., Cayan, D.R., Swetnam, T.W., 2006. Warming and earlier spring increase western U.S. forest wildfire activity. Science 313, 940–943.

Whitlock, C., Shafer, S.L., Marlon, J., 2003. The role of climate and vegetation change in shaping past and future fire regimes in the northwestern US and the implications for ecosystem management. Forest Ecol. Manage. 178, 5–21.

Wotton, B.M., Martell, D.L., 2005. A lightning fire occurrence model for Ontario. Can. J. Forest Res. 35, 1389–1401. http://dx.doi.org/10.1139/X05-071.

Wotton, B.M., Nock, C.A., Flannigan, M.D., 2010. Forest fire occurrence and climate change in Canada. Int. J. Wildland Fire 19, 253–271.

Xanthopoulos, G., Maheras, G., Gouma, V., Gouvas, M., 2006. Is the Keetch–Byram drought index (KBDI) directly related to plant water stress? Forest Ecol. Manage. 234 (Suppl. 1), S27.

Please cite this article in press as: Liu, Y., et al. Future U.S. wildfire potential trends projected using a dynamically downscaled climate change scenario. Forest Ecol. Manage. (2012), http://dx.doi.org/10.1016/j.foreco.2012.06.049